



ELSEVIER

Available online at www.sciencedirect.com

SCIENCE @ DIRECT®

Journal of Computational and Applied Mathematics 192 (2006) 445–459

JOURNAL OF
COMPUTATIONAL AND
APPLIED MATHEMATICS

www.elsevier.com/locate/cam

A comparison of numerical models for one-dimensional Stefan problems

E. Javierre*, C. Vuik, F.J. Vermolen, S. van der Zwaag¹

Delft University of Technology, 2628 CD Delft, Netherlands

Received 11 August 2004

Abstract

In this paper, we present a critical comparison of the suitability of several numerical methods, level set, moving grid and phase field model, to address two well-known Stefan problems in phase transformation studies: melting of a pure phase and diffusional solid-state phase transformations in a binary system. Similarity solutions are applied to verify the numerical results. The comparison shows that the type of phase transformation considered determines the convenience of the numerical techniques. Finally, it is shown both numerically and analytically that the solid–solid phase transformation is a limiting case of the solid–liquid transformation.

© 2005 Elsevier B.V. All rights reserved.

MSC: 35R35; 65M06; 80A22

Keywords: Stefan problem; Phase transformations; Similarity solutions; Moving grid method; Level set method; Phase field method

1. Introduction

In Stefan problems, the boundary of the domain has to be found as part of the solution. These problems describe several phenomena in nature, science and society, among others the melting of the polar ice caps, originally studied by J. Stefan, the dendritic solidification problem [4,12,21], the decrease of oxygen in a muscle in the vicinity of a clotted bloodvessel [5], the etching problem [26], the American option pricing

* Corresponding author.

E-mail address: e.javierre@ewi.tudelft.nl (E. Javierre).

¹ The authors want to thank the Dutch Technology Foundation (STW) for its financial support.

problem [10], or the phase transformations in metallic alloys [22]. This paper deals with a survey of existing numerical techniques for solving one-dimensional problems. In particular, we consider the melting problem and a solid-state phase transformation in parallel due to the resemblance in their governing equations, that we will show afterwards. Existence of a solution was proved in [6], while the uniqueness was proved in [7]. Moreover, the solution of the Stefan problems we consider here satisfies the maximum principle in each phase. Further, it is possible to derive analytical expressions for the solution of these problems in an infinite or semi-infinite one-dimensional-space. Under these hypotheses the solution is a function of $(x - s_0)/\sqrt{t}$ as proved by Hill [11], and it is often called the similarity solution.

Several numerical methods have been developed to solve various Stefan problems. Crank [5] provides a good introduction to the Stefan problems and presents an elaborate collection of numerical methods used for these problems. Front tracking methods use an explicit representation of the interface. Juric and Tryggvason [12] used a fixed grid in space where some variables of the problem, i.e. temperature, were calculated, and a moving grid on the interface where the interface heat sources were computed. Information from the interface to the fixed grid was transferred via the immersed boundary method. Segal et al. [22] used an adaptive grid method in which the movement of the grid was introduced into the governing equations by the use of the total time derivative (also called Arbitrarily Lagrangian Eulerian–ALE–approach). Murray and Landis [14] compared an adapted grid procedure with a fixed grid, and showed that the adaptive grid method captures more accurately the interface position, whereas the fixed grid algorithm gives a more precise heat distribution in the whole domain.

On the other hand, implicit methods are the natural alternative to the front tracking methods. Within these implicit methods the most used are the enthalpy method, the level set method and the phase field method. In the enthalpy method (see [5] and [15, Chapter 9]) the enthalpy function is introduced. This function measures the total heat of the system, and it has a jump discontinuity at the interface given by the heat released (or absorbed) during the phase change. This discontinuity is helpful to determine the interface position. Although this method has been successfully applied to phase change problems in [16–18], it has only recently been generalized to solid-state phase transformations with a simple condition on the moving boundary, see Lam et al. [19] for further details.

The level set method has gained much popularity for solving moving boundary problems. Firstly introduced in [20], it has already been generalized to many problems [23,24]. The level set function captures the interface position as its zero level set, and it is advected by the introduction of a hyperbolic equation into the governing set of equations. The velocity field, used to advect the level set function, is quite different within the applications of the level set method. Sussman et al. [25] use the fluid velocity to simulate incompressible two-phase flows. Chen et al. [4] use advection equations to extend the interface velocity onto the whole domain in a solidification problem and Adalsteinsson and Sethian [1] use a procedure based on the fast marching methods to extend the front velocity in such a way that it does not destroy the distance function attribute of the level set function. In these last references the velocity field is used for a numerical purpose.

Finally, the phase field method is a widely used method for phase transformation problems. The domain is parameterized by the phase field function which equals a fixed constant in each phase, and varies rapidly, but smoothly, within these two values in the interface region. The phase transformation occurs inside this interface region, whose thickness is an artificial parameter of the model. There are several phase field models in the literature, but the most used are based on the Kobayashi potential (see [27] for phase transitions in binary alloys) or based on the Caginalp potential (see [13] for the classical melting Stefan problem). The Kobayashi potential is based on a fourth-order polynomial with fixed minima at $x = \pm 1$

coupled with a monotonically increasing function of the temperature to define the free energy functional, whereas the Caginalp potential uses a double-well potential measured by a parameter and a linear coupling with the temperature. Fabbri and Voller [8] compare these models in detail. In both studies a discretization with an adaptive grid is used where the interface position coincides with one grid node. In their numerical experiments they compare the solutions with a fixed grid solution, and the Kobayashi potential shows a better agreement with this last solution. In addition, an asymptotic analysis for the phase field models is required to check whether the phase field solution converges to the sharp interface problem and to determine the parameters that appear in the formulation of the model. This asymptotic analysis is already done in [2], where Caginalp proves the convergence to the Stefan and Hele-Shaw problems by taking the limit in the parameters in a convenient way. In order to solve the governing equations numerically, Caginalp and Lin [3] use a coarse grid where the temperature of the system was calculated and a fine grid for the phase field function. Mackenzie and Robertson [13] propose to use an adaptive mesh with a high resolution in the interface region. Schmidt [21] uses finite elements with local refinement in the vicinity of the interface to simulate dendritic growth.

An outline of the paper is as follows. The governing equations of both the melting problem and the solid-state phase transformation problem will be described in Section 2, together with the analytical expressions of the similarity solutions for infinite domains. The moving grid, level set and phase field methods will be presented in Section 3. Some numerical results will be given in Section 4 and the conclusions in Section 5.

2. The physical problems

In the present paper we consider two classical Stefan problems: the melting problem and the solid-state phase transformation problem in binary metallic alloys. In the melting problem we have a liquid phase in contact with a solid phase separated by the interface, where the temperature is the melting temperature. This problem is also called solid–liquid transformation. The heat transport through the interface causes its displacement. In the second problem a volume of constant composition is surrounded by a diffusive phase. In the interface between the particle and the diffusive phase a constant concentration is assumed, and the gradient of the concentration causes the movement of the interface. This problem is also called solid–solid transformation. Moreover, we can think that the solid–solid transformation is a particular case of a solid–liquid transformation with zero thermal diffusivity in the liquid phase.

We restrict ourselves to the one-dimensional problem. Hence, some physical features of these problems like the surface tension (i.e., the Gibbs–Thomson effect) are not incorporated here. The domain will be denoted by $\Omega = [0, l]$, where l denotes the length. This domain will be split into two phases, and the interface separating these phases will consist of only one point. Therefore, a function $s : \mathbb{R}^+ \rightarrow [0, l]$ will assign each time t the position of the interface at this time $s(t)$.

2.1. The melting problem: a solid–liquid transformation

We consider the domain $\Omega = [0, l]$, where we have a material that is in its liquid state in a certain region of Ω we call $\Omega_{\text{liq}}(t) = [0, s(t))$ and it is in its solid state in the rest of the domain $\Omega_{\text{sol}}(t) = \Omega \setminus \bar{\Omega}_{\text{liq}}(t) = (s(t), l]$. The point separating the liquid and the solid phases determines the position of the interface $s(t)$. We denote the temperature in the point x at time t by $u(x, t)$.

The governing equations for this problem are the heat equation in both the liquid and the solid phases

$$\frac{\partial u}{\partial t}(x, t) = \frac{\partial}{\partial x} \left(K_{\text{liq}} \frac{\partial u}{\partial x} \right), \quad x \in \Omega_{\text{liq}}(t), \quad (1)$$

$$\frac{\partial u}{\partial t}(x, t) = \frac{\partial}{\partial x} \left(K_{\text{sol}} \frac{\partial u}{\partial x} \right), \quad x \in \Omega_{\text{sol}}(t), \quad (2)$$

where K_{sol} and K_{liq} denote the thermal diffusivities in the solid and the liquid phase respectively, which involve the heat capacity, density and the heat conduction coefficient of the materials. In this study we assume them to be constant in time and position. The velocity v of the interface is given by the jump condition

$$Lv = K_{\text{sol}} \frac{\partial u}{\partial x}(x, t)|_{x \downarrow s(t)} - K_{\text{liq}} \frac{\partial u}{\partial x}(x, t)|_{x \uparrow s(t)}, \quad (3)$$

where L denotes the latent heat of solidification. Eq. (3) is frequently called the Stefan condition. At the interface we have the melting temperature, that we choose here to be zero without loss of generality:

$$u(s(t), t) = 0. \quad (4)$$

In this problem thermally insulated domains are considered. Hence, no heat fluxes through the boundaries of the domain Ω are allowed, which leads to the homogeneous Neumann boundary conditions

$$\frac{\partial u}{\partial x}(x, t) = 0, \quad x \in \partial\Omega. \quad (5)$$

We consider a piecewise constant initial heat distribution

$$u(x, 0) = \begin{cases} u_{\text{liq}} & \text{if } x \in \Omega_{\text{liq}} = [0, s_0), \\ 0 & \text{if } x = s_0, \\ u_{\text{sol}} & \text{if } x \in \Omega_{\text{sol}} = (s_0, l], \end{cases}$$

where u_{liq} and u_{sol} are constants, generally positive and negative, respectively, and s_0 denotes the initial position of the interface, i.e., $s_0 = s(0)$. For this problem the position of the interface s is a differentiable function. Therefore, the velocity of the interface (v in Eq. (3)) can be replaced by $ds/dt(t)$

$$L \frac{ds}{dt}(t) = K_{\text{sol}} \frac{\partial u}{\partial x}(x, t)|_{x \downarrow s(t)} - K_{\text{liq}} \frac{\partial u}{\partial x}(x, t)|_{x \uparrow s(t)}. \quad (6)$$

2.2. Phase transformations in binary alloys: solid–solid transformations

We consider the domain $\Omega = [0, l]$ that is composed by a particle whose domain is denoted by $\Omega_{\text{part}}(t) = [0, s(t))$ and a diffusive phase $\Omega_{\text{dp}}(t) = \Omega \setminus \bar{\Omega}_{\text{part}}(t) = (s(t), l]$. The point separating the particle and the diffusive phase represents the interface $s(t)$. We consider the concentration c of a certain material within Ω , and we assume this concentration to be constant within the particle. Therefore, we have the following

governing equations:

$$c(x, t) = c^{\text{part}}, \quad x \in \Omega_{\text{part}}(t), \tag{7}$$

$$\frac{\partial c}{\partial t}(x, t) = \frac{\partial}{\partial x} \left(D \frac{\partial c}{\partial x}(x, t) \right), \quad x \in \Omega_{\text{dp}}(t), \tag{8}$$

where D denotes the diffusivity inside the diffusive phase Ω_{dp} . The velocity of the interface v is derived from a mass balance through the interface which leads to

$$(c^{\text{part}} - c^{\text{sol}})v = D \frac{\partial c}{\partial x}(x, t)|_{x \downarrow s(t)}, \tag{9}$$

where c^{sol} is the interface concentration, that is, $c(s(t), t) = c^{\text{sol}}$. Further $c^{\text{part}} \neq c^{\text{sol}}$, to avoid an undefined velocity.

We assume that the domain Ω is isolated, and therefore there is no concentration transported out of the domain Ω

$$\frac{\partial c}{\partial x}(x, t) = 0, \quad x \in \partial\Omega. \tag{10}$$

We assume a piecewise initial concentration as follows:

$$c(x, 0) = \begin{cases} c^{\text{part}} & \text{if } x \in \Omega_{\text{part}} = [0, s_0), \\ c^{\text{sol}} & \text{if } x = s_0, \\ c^0 & \text{if } x \in \Omega_{\text{dp}} = (s_0, l], \end{cases}$$

where s_0 is the initial position of the interface, and $c^{\text{part}}, c^{\text{sol}}, c^0 > 0$. Under these hypotheses s is a monotonous and differentiable function. Hence, the Stefan condition for the velocity of the interface Eq. (9) can be expressed by

$$(c^{\text{part}} - c^{\text{sol}}) \frac{ds}{dt}(t) = D \frac{\partial c}{\partial x}(x, t)|_{x \downarrow s(t)}. \tag{11}$$

If we take the thermal diffusivity of the liquid phase zero in the melting problem and assign $L = c^{\text{part}} - c^{\text{sol}}$, then Eqs. (1)–(3) are equivalent to (7)–(9), being the only difference between the two models in the boundary value at the interface, that simply realizes a translation.

2.3. Similarity solutions

In our numerical experiments we will compare the solutions obtained from the different numerical methods with the analytical solutions that exist for the problems presented above. These solutions are expressed as functions of $(x - s_0)/\sqrt{t}$ as proved in [11], and the domain Ω has to be infinite or semi-infinite. Hence, for $\Omega = \mathbb{R}$ the interface position is given by $s(t) = s_0 + 2\alpha\sqrt{t}$, where the constant α is obtained by solving the following equation:

$$\alpha = \frac{\sqrt{K_{\text{sol}}}}{\sqrt{\pi}L} \frac{u_{\text{sol}}}{\text{erfc}\left(\frac{\alpha}{\sqrt{K_{\text{sol}}}}\right)} \exp\left(-\frac{\alpha^2}{K_{\text{sol}}}\right) + \frac{\sqrt{K_{\text{liq}}}}{\sqrt{\pi}L} \frac{u_{\text{liq}}}{2 - \text{erfc}\left(\frac{\alpha}{\sqrt{K_{\text{liq}}}}\right)} \exp\left(-\frac{\alpha^2}{K_{\text{liq}}}\right) \tag{12}$$

for the melting problem and

$$\alpha = \frac{c^0 - c^{\text{sol}}}{c^{\text{part}} - c^{\text{sol}}} \sqrt{\frac{D}{\pi}} \frac{\exp\left(-\frac{\alpha^2}{D}\right)}{\operatorname{erfc}\left(\frac{\alpha}{\sqrt{D}}\right)}, \quad (13)$$

for the solid–solid transformation problem. As we noted above, if we let $K_{\text{liq}} = 0$, $L = c^{\text{part}} - c^{\text{sol}}$ and identify u_{sol} with the concentration difference $c^0 - c^{\text{sol}}$, then Eqs. (12) and (13) are the same. When α is known, the temperature is given by

$$u(x, t) = \begin{cases} -\frac{u_{\text{liq}} \operatorname{erfc}(\alpha/\sqrt{K_{\text{liq}}})}{2 - \operatorname{erfc}(\alpha/\sqrt{K_{\text{liq}}})} + \frac{u_{\text{liq}} \operatorname{erfc}((x - s_0)/2\sqrt{K_{\text{liq}}t})}{2 - \operatorname{erfc}(\alpha/\sqrt{K_{\text{liq}}})}, & \text{if } x < s(t), \\ u_{\text{sol}} - \frac{u_{\text{sol}} \operatorname{erfc}((x - s_0)/2\sqrt{K_{\text{sol}}t})}{\operatorname{erfc}(\alpha/\sqrt{K_{\text{sol}}})}, & \text{if } x \geq s(t) \end{cases} \quad (14)$$

for the melting problem, whereas the concentration is given by

$$c(x, t) = \begin{cases} c^{\text{part}} & \text{if } x < s(t), \\ c^0 + \frac{(c^{\text{sol}} - c^0) \operatorname{erfc}((x - s_0)/2\sqrt{Dt})}{\operatorname{erfc}(\alpha/\sqrt{D})}, & \text{if } x \geq s(t) \end{cases} \quad (15)$$

for the solid–solid transformation problem.

3. The numerical solution methods

In this section we present three numerical methods to solve the solid–liquid and the solid–solid transformations. These are the moving grid, the level set and the phase field methods. The moving grid method, as presented here, is easy to implement and to increase the order of accuracy in the discretizations. Moreover, it leads to symmetric matrices, which are desirable to solve the large systems of equations numerically. For higher-dimensional methods it is convenient to introduce the displacement of the grid into the governing equations (ALE approach). However, an implicit discretization of the convection term will lead to a nonsymmetric matrix. The level set method captures the interface position implicitly and moves it according to a new artificial equation in the governing mathematical model. It is known from literature that merging interfaces are easy to handle with the level set method. In addition, for this method a fixed grid can be used, which avoids the mesh generation at every time step required with the moving grid. Finally, the phase field method allows a better agreement between the numerical model and the physical problem, since most of the driving forces acting on the interface (such as surface tension) are related to the phase field parameters. However, an adaptive mesh with a local refinement in the interfacial region seems to be necessary.

For the sake of simplicity we will restrict the presentation of the numerical methods considered in this paper to the solid–liquid transformations. Generalization of these procedures to the solid–solid transformations is straightforward, except for the phase field model.

3.1. The moving grid method

Here we present an interpolative moving grid method, in which the grid is computed for each time step and the solution is interpolated from the old grid to the new grid. The interpolation might be abolished by the introduction of the grid displacement into the governing equations with the ALE approach. This technique is used in [14,22]. However, we prefer to use interpolation for the ease of implementation and since the difference is not decisive for 1D problems.

Let N be the total number of grid intervals, r of those lie inside the liquid phase and $N - r$ lie inside the solid phase. The grid is uniform in each phase and the interface is always located in the r th node. Due to the movement of the interface, the grid should be adapted at each time step. To obtain the temperature at the next time step, a backward Euler scheme is used for the time discretization of the heat equation and central differences are used for the discretization in space. With the temperature profile, the displacement of the interface is calculated using first-order accurate directional derivatives in each phase, and the grid is adapted to the new position of the interface. Finally, the solution is interpolated from the previous grid to the new one. The interested reader is referred to [5] for further details.

3.2. The level set method

The level set method captures the position of the interface as the zero-level set of a continuous function ϕ initialized as a distance function,

$$\phi(x, 0) = \begin{cases} |x - s_0| & \text{if } x < s_0, \\ 0 & \text{if } x = s_0, \\ -|x - s_0| & \text{if } x > s_0, \end{cases}$$

which has been arbitrarily selected positive in the liquid phase. This function is called the level set function, and the interface is implicitly represented by its zero-level set

$$x = s(t) \Leftrightarrow \phi(x, t) = 0, \quad \forall t \geq 0.$$

The evolution of the level set function is derived from the above equation taking into account a continuous extension v of the interface velocity (6) (or (11), respectively) as follows:

$$\frac{\partial \phi}{\partial t}(x, t) + v(x, t) \frac{\partial \phi}{\partial x}(x, t) = 0, \quad x \in \Omega. \quad (16)$$

In our specific application, the interface velocity is only defined at the front position itself. Hence, a continuous extension v of the interface velocity is unavoidable, and it is taken as the steady solution of the next advection equation

$$\frac{\partial \tilde{v}}{\partial \tau}(x, \tau) + S\left(\phi(x, t) \frac{\partial \phi}{\partial x}(x, t)\right) \frac{\partial \tilde{v}}{\partial x}(x, \tau) = 0 \quad (17)$$

that propagates the front velocity in the correct upwind direction (see [4]). Here τ denotes a fictitious time step not related to the main time step, and S denotes the sign function.

For general dimensions, the normal vector to the interface is given by $\mathbf{n} = \nabla \phi / |\nabla \phi|$ and the curvature of the interface by $\kappa = \nabla \cdot \mathbf{n}$. Furthermore, several simplifications can be done when ϕ is signed distance function (see [24] for further details). However, after solving (16) the level set function ϕ possibly is no

longer a distance function. Then, a reinitialization procedure is required. This reinitialized level set is the steady-state solution of

$$\frac{\partial \tilde{\phi}}{\partial \tau}(x, \tau) = S(\phi(x, t)) \left(1 - \left| \frac{\partial \tilde{\phi}}{\partial x}(x, \tau) \right| \right), \quad (18)$$

where τ is again a fictitious time and $\phi(x, t)$ is the level set we want to set as a distance function. Note that the zero-level set of ϕ is not changed, and $|\partial \tilde{\phi} / \partial x| = 1$, which characterizes the distance functions, in the steady solution.

The numerical discretization of the set of governing equations is done on a uniform fixed grid with grid spacing Δx . The front velocity is calculated by forward differences in the solid phase and backward differences in the liquid phase. The extension of the front velocity and the advection of the level set function are done by a forward Euler scheme for the time discretization and an upwind discretization in space. This leads to stability conditions for the time steppings: $\Delta \tau < \Delta x$ in the artificial advection of the front velocity, and $\max_{x \in \Omega} |v(x, t)| \Delta t / \Delta x < 1$ in the advection of the level set function. The equation for the reinitialization is discretized by the first-order accurate Godunov's scheme presented in [25]. The heat equation is discretized using a backward Euler scheme in time and central differences in space. For the neighbouring nodes to the interface we use the second-order derivatives of the quadratic Lagrangian interpolation polynomials that approximate the solution in the vicinity of the interface from the appropriate side of the interface. When a grid node changes phase (i.e. the interface crosses it) the discretization of the heat equation should be adapted. When this happens, the node in question is not included in the discretization, and the solution at this node is obtained by interpolation from the neighboring nodes within the same phase. This procedure is slightly different from the method presented recently in [9], where the temperature in the conflictive node is adapted to the interface position before the heat equation is solved.

3.3. The phase field method

The phase field method uses a function $\phi(x, t)$ which characterizes the phase of the system at each point x and time t . This function, that is called the phase field function, assumes an interface region of thickness ε where the phase transitions occur. This is clearly different from the moving grid and level set methods where a sharp interface is considered. The phase field function ϕ is given by

$$\phi(x, t) = \begin{cases} 1 & \text{if } x \text{ is in the liquid phase at time } t, \\ -1 & \text{if } x \text{ is in the solid phase at time } t \end{cases}$$

and the interface region is characterized by $-1 < \phi(x, t) < 1$. Then the evolution of the system is described by the following system of two coupled partial differential equations:

$$v_{\xi}^2 \frac{\partial \phi}{\partial t} = - \frac{\delta \mathcal{F}}{\delta \phi},$$

$$\frac{\partial u}{\partial t} + \frac{L}{2} \frac{\partial \phi}{\partial t} = \frac{\partial}{\partial x} \left(K \frac{\partial u}{\partial x} \right),$$

where K is the appropriate diffusivity constant in each phase, i.e., $K = K_{\text{liq}}$ where $\phi > 0$ and $K = K_{\text{sol}}$ where $\phi < 0$. Further, L denotes the latent heat and \mathcal{F} denotes a free energy functional which is a function

of ϕ as well as other variables of the problem, and $\delta\mathcal{F}/\delta\phi$ denotes the variational derivative of \mathcal{F} with respect to ϕ . The parameter ν is a relaxation time and ξ is related with the thickness of the interface region. We use the Caginalp model, for which the asymptotic analysis is done in [2]. The free energy functional \mathcal{F} is expressed by

$$\mathcal{F}(\phi, u) = \int_{\Omega} \left[\frac{1}{2} \xi^2 \left(\frac{\partial\phi}{\partial x} \right)^2 + f(\phi, u) \right] dx,$$

where f is the so-called free energy density which consists of a double-well potential measured by a parameter a and a term coupling u with ϕ

$$f(\phi, u) = \frac{1}{8a} (\phi^2 - 1)^2 - 2u\phi.$$

The two minima of f establish the stable states of the problem (i.e. the liquid and solid-states), which are slightly displaced from its physical values $\phi = \pm 1$ due to the influence of the parameter a . Hence to minimize this influence the parameter a should be chosen small. Further, the interface thickness is given by the relation $\varepsilon = \xi\sqrt{a}$.

The phase field varies rapidly from -1 to 1 within the interface region, which motivates the use of an adaptive mesh procedure. Here the approach presented in [13] is used. The adaptive mesh is constructed by an equidistribution principle

$$\int_{x_i(t)}^{x_{i+1}(t)} M(\tilde{x}, t) d\tilde{x} = \frac{1}{N} \int_0^1 M(\tilde{x}, t) d\tilde{x} \quad \text{for } i = 0, 1, \dots, N - 1, \tag{19}$$

where N is the number of space intervals we consider in our spatial domain Ω and M is a monitor function related with the thickness of the interfacial region. In this case

$$M(x, t) = \gamma\beta(t) + \operatorname{sech} \left(\frac{x - s(t)}{2\varepsilon} \right), \quad \beta(t) = \int_0^1 \operatorname{sech} \left(\frac{x - s(t)}{2\varepsilon} \right) dx, \tag{20}$$

where $\gamma > 0$ is a parameter chosen by the user. The parameter γ must be chosen positive to ensure that the monitor function M is positive and not zero to avoid the clustering of all the grid nodes inside the interface region, since the number of grid nodes placed within the interface region is approximately $N/1 + \gamma$.

Finally, the use of the Caginalp potential and the adaptive mesh procedure leads to the following system of differential equations:

$$\nu\xi^2 \left(\frac{D\phi}{Dt} - \frac{dx}{dt} \frac{\partial\phi}{\partial x} \right) = \xi^2 \frac{\partial^2\phi}{\partial x^2} - \frac{1}{2a} (\phi^3 - \phi) + 2u, \tag{21a}$$

$$\frac{Du}{Dt} - \frac{dx}{dt} \frac{\partial u}{\partial x} + \frac{L}{2} \left(\frac{D\phi}{Dt} - \frac{dx}{dt} \frac{\partial\phi}{\partial x} \right) = \frac{\partial}{\partial x} \left(K \frac{\partial u}{\partial x} \right), \tag{21b}$$

where the total-time derivative (ALE approach, see also Section 3.1) has been used to incorporate the mesh movement into the governing equations. These equations are solved separately. It has to be remarked that the mesh at the new time step is required to solve system (21). We use the following algorithm. First, we estimate the interface position at the new time step by $s^{n+1} = 2s^n - s^{n-1}$. Note that a fixed time step is

used. Then, the mesh at the new time step is calculated with the equidistribution principle Eqs. (19)–(20), which is determined by solving the nonlinear equation

$$\begin{aligned} \gamma\beta(t^{n+1})x_i^{n+1} + 2\varepsilon \left[\sin^{-1} \left(\tanh \left(\frac{x_i^{n+1} - s^{n+1}}{2\varepsilon} \right) \right) - \sin^{-1} \left(\tanh \left(\frac{-s^{n+1}}{2\varepsilon} \right) \right) \right] \\ = \frac{i\beta(t^{n+1})(\gamma + 1)}{N} \end{aligned}$$

for x_i^{n+1} , $i=0, \dots, N$. Thereafter, the phase field at the new time step is calculated from Eq. (21a), where the temperature at the previous time step is used. For the computation of the phase field function, we use the following discretization:

$$\begin{aligned} v\xi^2 \left(\frac{\phi_i^{n+1} - \phi_i^n}{\Delta t} - \frac{x_i^{n+1} - x_i^n}{\Delta t} \frac{\phi_{i+1}^n - \phi_{i-1}^n}{h_{i+1}^n + h_i^n} \right) = \frac{2\xi^2}{h_{i+1}^{n+1} + h_i^{n+1}} \left(\frac{\phi_{i+1}^{n+1} - \phi_i^{n+1}}{h_{i+1}^{n+1}} - \frac{\phi_i^{n+1} - \phi_{i-1}^{n+1}}{h_i^{n+1}} \right) \\ - \frac{1}{2a} [(\phi_i^{n+1})^3 - \phi_i^{n+1}] + 2u_i^n \end{aligned}$$

for $i = 1, \dots, N - 1$. The value at the boundary nodes is given by the boundary conditions. We use the Newton method to solve this nonlinear system of equations up to a given tolerance. Subsequently, the temperature distribution is obtained by substitution of the phase field at the new time step into its time derivative in Eq. (21b). We use the following discretization

$$\begin{aligned} \frac{u_i^{n+1} - u_i^n}{\Delta t} - \frac{x_i^{n+1} - x_i^n}{\Delta t} \frac{u_{i+1}^n - u_{i-1}^n}{h_{i+1}^n + h_i^n} + \frac{L}{2} \left(\frac{\phi_i^{n+1} - \phi_i^n}{\Delta t} - \frac{x_i^{n+1} - x_i^n}{\Delta t} \frac{\phi_{i+1}^n - \phi_{i-1}^n}{h_{i+1}^n + h_i^n} \right) \\ = \frac{2}{h_{i+1}^{n+1} + h_i^{n+1}} \left(K_{i+1/2}^{n+1} \frac{u_{i+1}^{n+1} - u_i^{n+1}}{h_i^{n+1}} - K_{i-1/2}^{n+1} \frac{u_i^{n+1} - u_{i-1}^{n+1}}{h_i^{n+1}} \right) \end{aligned}$$

for $i = 1, \dots, N - 1$. The value at the boundary nodes is obtained from the boundary conditions. Note that central differences have been used to discretize the convective terms since the phase transformation is diffusion controlled. We refer the interested reader to [13] for further details. In the post-processing of the results, the interface position is calculated as the zero of the phase field function by linear interpolation.

In addition, Mackenzie and Robertson [13] study the existence of a solution for the nonlinear system coming from Eq. (21a). They found a sufficient condition for the existence of a numerical solution based on the time step: $\Delta t < 2va\xi^2 = 2v\varepsilon^2$, which reveals the numerical difficulties that arise when we try to recover the sharp interface problem with ε small. However, in their and our numerical experiments it is possible to use a larger time step, although its selection is very sensitive to the other parameters in the phase field model.

4. Numerical results

In this section, we present some numerical results for both the single phase (solid–solid transformation) and the two phases (solid–liquid transformation) problems. Our aim is to mimic the first Stefan problem

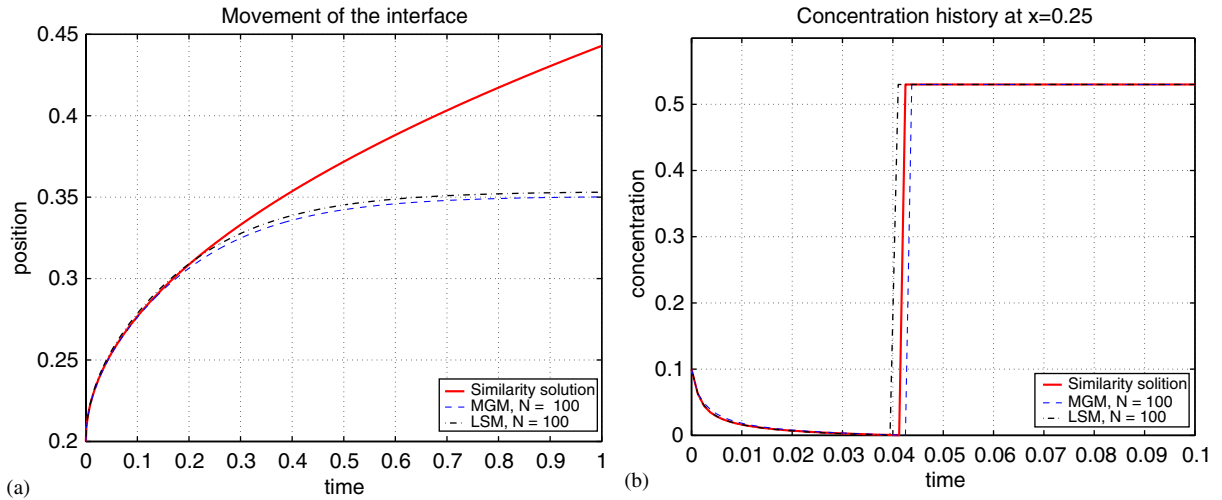


Fig. 1. The solid–solid transformation problem with the moving grid (MGM) and the level set (LSM) methods. (a) Interface position vs. time, (b) concentration history at $x = 0.25$.

by solving the second Stefan problem, for which the phase field method can be applied. We also examine the convergence of the moving grid and the level set methods for the single-phase problem. The data used through all the computations are: the concentration inside the particle $c^{\text{part}} = 0.53$, the concentration on the interface $c^{\text{sol}} = 0$, the initial concentration in the diffusive phase $c^0 = 0.1$, the diffusivity constant $D = 1$, the domain length $l = 1$ and the initial position of the interface $s_0 = 0.2$.

4.1. Solid–solid transformation

In this section, we use the moving grid and the level set methods to simulate the single-phase problem presented above.

In Fig. 1(a) the evolution of the interface positions for the moving grid, the level set methods and the similarity solution (obtained from Eq. (13)) is shown. It appears that there is a close agreement with the similarity solution in the beginning of the simulation. However, in the numerical simulations a finite domain Ω is considered whereas for the similarity solution the domain Ω is infinite. This causes the divergence of the numerical solutions with respect to the similarity solution if time evolves. In Fig. 1(b) the concentration at $x = 0.25$ vs. the time is compared again with the similarity solution given by Eq. (15). For both the moving grid and the level set methods we take $N = 100$. For the moving grid method the time step is $\Delta t = 1.25 \times 10^{-3}$, whereas in the level set method the time step is determined by the CFL condition for stability, which prescribes $\Delta t^n = \text{CFL} \cdot \Delta x / |v^n|$ with $\text{CFL} < 1$. In our calculations we have used $\text{CFL} = 0.1$. This choice made the time step to vary from 2.918×10^{-4} to 1.25×10^{-3} , which was used as an upper bound to avoid excessively large times steps due to small interface velocities.

In Table 1 the convergence to the similarity solution of both the moving grid and the level set methods is examined, with final time for the numerical integration $t_{\text{end}} = 0.1$. The time step was refined when N was increased in both methods. First-order convergence in the interface position is observed for both methods, although a slightly higher accuracy is observed with the moving grid method. This is likely due to the differences in the grid spacing and time steppings for both methods.

Table 1

Convergence analysis for the moving grid method (left) and the level set method (right)

N	Moving grid method		Level set method	
	$s_h(0.1)$	$\ s - s_h\ _\infty$	$s_h(0.1)$	$\ s - s_h\ _\infty$
100	0.276223	0.000727	0.278445	0.001630
200	0.276470	0.000495	0.277812	0.000997
400	0.276609	0.000343	0.277405	0.000594
800	0.276687	0.000239	0.277144	0.000342
1600	0.276730	0.000168	0.276988	0.000194

Similarity solution $s(0.1) = 0.276815$.

Table 2

Values of α for different values of K_{liq}

K_{liq}	0.05	0.01	0.005	0
α	0.169082	0.127968	0.122595	0.121455

4.2. Solid–liquid transformation

In this section, we mimic the problem presented above with a solid–liquid transformation problem. Hence, we consider the next initial temperature distribution

$$u(x, 0) = \begin{cases} 0.53 & \text{in the liquid phase } (0 \leq x < s_0), \\ 0 & \text{on the interface } x = s_0, \\ 0.1 & \text{in the solid phase } (s_0 < x \leq 1), \end{cases}$$

where the initial position of the interface is $s_0 = 0.2$ again. The latent heat $L = c^{\text{part}} - c^{\text{sol}} = 0.53$ and the thermal diffusivity in the solid phase is $K_{\text{sol}} = D = 1$ and in the liquid phase is either $K_{\text{liq}} = 0.05$, 0.01 or 0.005. As mentioned in Section 2.3, the interface position of the similarity solution is determined by a parameter α which is calculated from the initial data in Eq. (12). In Table 2 values of α are given for different values of K_{liq} , compared with the value of α in the solid–solid transformation problem Eq. (13). Note that the solid phase has been artificially super-heated to mimic the solid–solid phase transformation problem presented above, which is obtained for $K_{\text{liq}} = 0$. The three methods were also tested on classical Stefan problems, and the same kind of behavior for the numerical solutions as presented here has been observed.

In Fig. 2(a) the interface position with the moving grid, the level set and the phase field methods is presented. Comparison with the similarity solution is only correct for small times, due to the bounded domain. Hence $t_{\text{end}} = 0.25$ is used as the final time for the simulation. In Fig. 2(b) the temperature history in $x = 0.25$ is presented, and the numerical solutions are consistent with the similarity solution given by Eq. (14). For the moving grid method $N = 200$ grid intervals were used for the entire domain Ω , of which $r = 100$ were in the liquid phase. The time step used was $\Delta t = 5 \times 10^{-4}$. For the level set method we took $N = 200$, while the CFL parameter was 0.1. The time step varied from 9.2398×10^{-5} to 5×10^{-4} , which was used as an upper bound. Finally, for the phase field method $a = 0.0625$ and

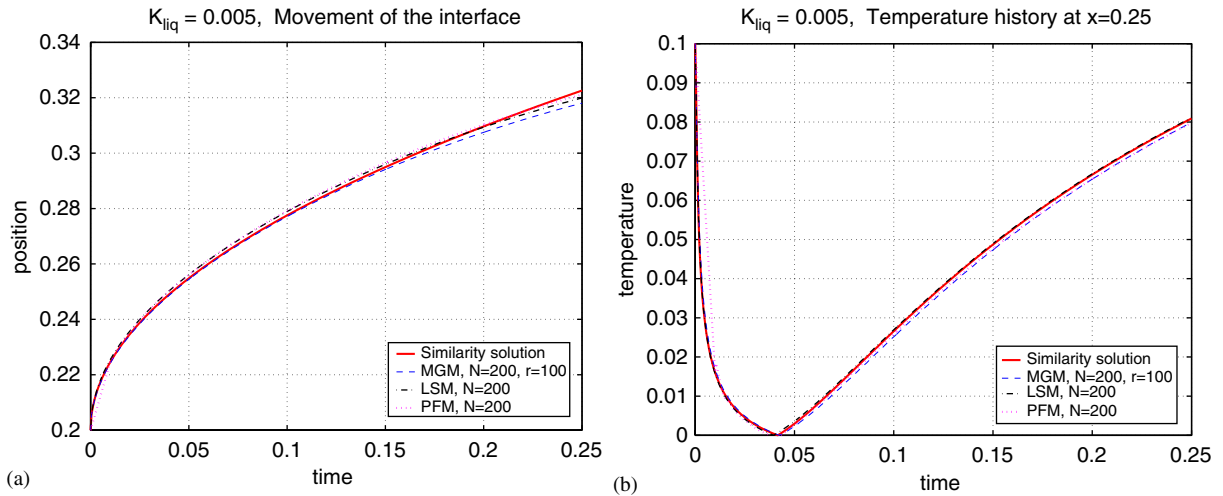


Fig. 2. The solid–liquid transformation problem with the moving grid, the level set and the phase field methods. (a) Interface position vs. time, (b) temperature history at $x = 0.25$.

$\xi = 0.0001$, which led to an interface thickness of $\varepsilon = 5 \times 10^{-5}$ and relaxation time $\nu = 1$. Further we use $N = 200$ and $\gamma = 1$, which implies that about 100 nodes were placed within the interface region. As mentioned in Section 3.3, the criterion on the time stepping found in [13] leads to $\Delta t < 1.2510^{-9}$ which is useless for practical purposes. However, as they also pointed in [13] it has been possible to obtain satisfactory results with larger time steps. In this case we used $\Delta t = 5 \times 10^{-4}$. The initial temperature distribution was obtained from the similarity solution Eq. (14) using an initial time $t_0 = 0.01$, since it was seen that a discontinuous initial temperature distribution causes instabilities in the phase field method. The same experiment has been done for $K_{liq} = 0.05$ and 0.01 , for which $\xi = 0.002$ and 0.0002 were used, respectively. The following observations can be done: decreasing the interface thickness might require to decrease the time step (although in our calculations $\Delta t = 5 \times 10^{-4}$ was used and satisfactory results were obtained), decreasing the diffusivity K_{liq} will require to increase the initial time t_0 to obtain an initial temperature distribution that is sufficiently smooth inside the interface region. Further decreasing the thermal diffusivity K_{liq} requires a decrease of the interface thickness.

5. Conclusions

In this paper, we consider two Stefan problems resulting from phase transformations: the melting problem and a diffusional phase transformation in binary alloys where only in one of the two phases the solution of the diffusion equation is determined, whereas the solution is constant in the other phase. Numerical solutions of those problems have been obtained with the moving grid, the level set and the phase field methods.

The formulation of the problems and the existing similarity solutions show the resemblance between the two problems. In fact, the diffusional one phase transformation is a special case of the melting problem.

From the numerical computations several conclusions can be obtained:

- Both the moving grid and the level set methods are suitable numerical models for the solid-state phase transformation, and their accuracy is comparable.
- The same can be concluded for the melting problem. Furthermore, for this problem the phase field method is also suitable. From the reported results (Fig. 2) one might conclude that the phase field method gives a better approximation of the interface position and temperature profile. However, the grid resolution within the interfacial region is much higher with the phase field method than with the moving grid and the level set methods, which also leads to larger computational cost.
- The phase field method has shown to be applicable for the melting problem, even when the difference of the thermal properties in each phase is remarkable. Unfortunately it is hard to derive appropriate phase field parameter values from the physical parameters of the phases involved, which limits the true predictive power of this technique. The moving grid and the level set methods do not suffer from this high dependence of the physical parameters of the problem. Their input values can be obtained rather easily from tables and phase diagrams.

The interpolative approach presented for the moving grid method can be replaced by the ALE approach, which introduces the displacement of the grid into the governing equations, leading to solving a convection-diffusion equation, which is more convenient for higher-dimensional problems. Topological changes, which involve merging or breaking of the interface, are difficult to model with the moving grid method. However, this is easily handled in the level set method. The difficulties in the level set method are the extension of the front velocity and the reinitialization, although they can be overcome without much effort. This motivates us to investigate the level set method for higher dimensional problems.

References

- [1] D. Adalsteinsson, J.A. Sethian, The fast construction of extension velocities in level set methods, *J. Comput. Phys.* 148 (1999) 2–22.
- [2] G. Caginalp, Stefan and Hele-Shaw type models as asymptotic of the phase field equations, *Phys. Rev. A* 39 (1989) 5887–5896.
- [3] G. Caginalp, J.T. Lin, A numerical analysis of an anisotropic phase field model, *IMA J. Appl. Math.* 39 (1987) 51–66.
- [4] S. Chen, B. Merriman, S. Osher, P. Smereka, A simple level set method for solving Stefan problems, *J. Comput. Phys.* 135 (1997) 8–29.
- [5] J. Crank, *Free and Moving Boundary Problems*, Clarendon Press, Oxford, 1984.
- [6] G.W. Evans, A note on the existence of a solution to a problem of Stefan, *Q. Appl. Math.* 9 (1951) 185–193.
- [7] J. Douglas, A uniqueness theorem for the solution of a Stefan problem, *Proc. Am. Math. Soc.* 8 (1957) 402–408.
- [8] M. Fabbri, V.R. Voller, The phase field method in the sharp-interface limit: a comparison between model potentials, *J. Comput. Phys.* 130 (1997) 256–265.
- [9] F. Gibou, R. Fedkiw, R. Caflisch, S. Osher, A level set approach for the numerical simulation of dendritic growth, *J. Sci. Comput.* 19 (2003) 183–199.
- [10] J. Goodman, D.N. Ostrov, On the early exercise boundary of the American put option, *SIAM J. Appl. Math.* 62 (2002) 1823–1835.
- [11] J.M. Hill, *One-Dimensional Stefan Problems: An Introduction*, Longman Scientific Technical, Harlow, 1987.
- [12] D. Juric, G. Tryggvason, A front-tracking method for dendritic solidification, *J. Comput. Phys.* 123 (1996) 127–148.
- [13] J.A. Mackenzie, M.L. Robertson, A moving mesh method for the solution of the one-dimensional phase field equations, *J. Comput. Phys.* 181 (2002) 526–544.

- [14] W.D. Murray, F. Landis, Numerical and machine solutions of transient heat-conduction problems involving melting or freezing, *Trans. ASME (C) J. Heat Transfer* 81 (1959) 106–112.
- [15] W.J. Minkowycz, E.M. Sparrow, *Advances in Numerical Heat Transfer*, vol. 1, Taylor & Francis, Washington, 1997.
- [16] V.R. Voller, M. Cross, Accurate solutions of moving boundary problems using the enthalpy method, *Int. J. Heat Mass Transfer* 24 (1981) 545–556.
- [17] V.R. Voller, An implicit enthalpy solution for phase change problems: with application to a binary alloy solidification, *Appl. Math. Modell.* 11 (1987) 110–116.
- [18] B. Nedjar, An enthalpy-based finite element method for nonlinear heat problems involving phase change, *Comput. Struct.* 80 (2002) 9–21.
- [19] Y.C. Lam, J.C. Chai, P. Rath, H. Zheng, V.M. Murukeshan, A fixed-grid method for chemical etching, *Int. Commun. Heat Mass Transfer* 31 (2004) 1123–1131.
- [20] S. Osher, J.A. Sethian, Fronts propagating with curvature-dependent speed: algorithms based on Hamilton–Jacobi formulations, *J. Comput. Phys.* 79 (1988) 12–49.
- [21] A. Schmidt, Computation of three dimensional dendrites with finite elements, *J. Comput. Phys.* 125 (1996) 293–312.
- [22] G. Segal, C. Vuik, F. Vermolen, A conserving discretization for the free boundary in a two-dimensional Stefan problem, *J. Comput. Phys.* 141 (1998) 1–21.
- [23] J.A. Sethian, *Level Set Methods and Fast Marching Methods*, Cambridge University Press, New York, 1999.
- [24] S. Osher, R. Fedkiw, *Level Set Methods and Dynamic Implicit Surfaces*, Springer, New York, 2003.
- [25] M. Sussman, P. Smereka, S. Osher, A level set approach for computing solutions to incompressible two-phase flow, *J. Comput. Phys.* 114 (1994) 146–159.
- [26] C. Vuik, C. Cuvelier, Numerical solution of an etching problem, *J. Comput. Phys.* 59 (1985) 247–263.
- [27] A.A. Wheeler, W.J. Boettinger, G.B. McFadden, Phase field model for isothermal phase transitions in binary alloys, *Phys. Rev. A* 45 (1992) 7424–7439.